Generalization of the Dual Frequency Method of Multipath Calibration for Global Reference Networks

R. Benjamin Harris and E. Glenn Lightsey
Department of Aerospace Engineering and Engineering Mechanics, The University of Texas at Austin

BIOGRAPHY

Mr. Harris is an Engineering Scientist at Applied Research Laboratories, The University of Texas at Austin (ARL:UT). His professional focus is the development of systems to monitor and control spacecraft, primarily telecommunication and navigation satellites. Mr. Harris is also member of the GPS Toolkit (GPSTk) team. Mr. Harris obtained a B.S. in Aerospace Engineering from the University of Texas at Austin in 1994, where he is now a Ph.D. candidate in the same department. In addition, he received an M.S. in Aeronautics and Astronautics from Stanford University in 2000.

Dr. E. Glenn Lightsey is an Associate Professor in the Department of Aerospace Engineering and Engineering Mechanics at the University of Texas at Austin. He specializes in the dynamics and control of vehicles using avionics sensors such as the Global Positioning System for navigation and attitude determination. Dr. Lightsey worked at NASA's Goddard Space Flight Center for 13 years. He received his Ph.D. from Stanford University in 1997. He has authored over 20 technical publications on the dynamics and control of vehicles using sensors such as GPS.

ABSTRACT

The Dual Frequency Method, or DFM, creates a model of multipath at static reference stations. The DFM uses a combination of pseudorange and carrier phase observations to both isolate multipath and remove the influence of the ionosphere delay. The method also includes spatial processing that removes biases introduced by use of carrier phase observations.

The DFM can be extended in two fundamental ways. First, the original formulation of the DFM describes how to isolate multipath for pseudorange minus carrier phase multipath on L1. The DFM can also be applied to a number of other observation combinations. More combinations are possible using the new civilian GPS signal, L2C. An application that is part of the GPS Toolkit (GPSTk) provides a means to both apply and explore the family of multipath combinations.

Any linear combination of range-type observables will contain a bias, derived from the observables involved. Not only carrier phase observables but also pseudorange observables contain biases. The DFM describes a processing technique for removing the biases when the linear combinations are organized by overhead pass. The technique requires finding the intersections of the passes. Prior investigations have numerically computed the intersections. An analytic solution to that search exists that is based on simplified dynamics of the GPS satellites. The analytic solution not only finds intersections for passes relative to given site's overhead passes, but also generally for any site on the surface of the Earth. The analytic solution has the potential to produce intersection solutions that agree with the numerical solution to within fractions of a degree, when measured with azimuth and elevation. However that difference can grow large to even 2 degrees as satellites vary from the nominal GPS orbit.

BACKGROUND

Multipath occurs when reflections of an electromagnetic wave interfere with the line-of-sight (LOS) wave. Because the antennas that track GPS are typically omnidirectional, multipath is a primary mode of error for its measurements. Multipath interference corrupts the signals on both the GPS frequencies, L1 and L2. Figure 1 depicts how multipath is generated in the local environment. Both the direct and reflected signals carry time codes; the receiver must track these codes to estimate the relative time delay and phase offset to the GPS satellite. However, multipath signals corrupt the code tracking, skewing the code correlation processes. The skewed correlation results in errors in all products of the receiver, including the pseudorange and carrier phase.

It is possible to mitigate multipath using hardware. The

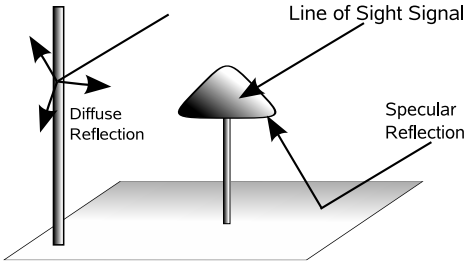

Fig. 1 Modes of multipath error.

antenna receive pattern can be shaped to amplify LOS signals [1]. In addition a *choke ring* can be used to reduce the amplitude of multipath reflections that travel through free space to reach the antenna. Within the receiver, the correlation process can strengthened [2, 3]. However, because the correlation process within a receiver works with a limited number of correlators that process current samples without knowledge of the future samples, then the performance of such alternate correlators is fundamentally bounded [4].

Other multipath mitigation approaches can be applied to measurements after those measurements are generated by a receiver. One class of corrections can be used when the reflections can be predicted. Reflections from large flat bodies generate reflections that are coherent–that is, the reflected wave is similar to the LOS wave, with a constant change in phase, amplitude and delay. These reflections can be simulated as if they were optical reflections. This mode of reflection is referred to as *specular reflection*. When those waves travel through free space, they can be modeled using the Geometric Theory of Diffraction (GTD). Researchers have successfully used the GTD to predict the effect of multipath on observations when a receiver is in a controlled environment.[5] Furthermore, predictive models have been used to compensate for multipath in environments where all nearby reflectors are specular and can be rigorously modeled, such as in the space environment [6].

Often receivers are deployed in complex or remote environments for which it is prohibitive or difficult to create and maintain a model. However when those environments do not change from day to day, then multipath they cause is simply a function of the relative geometry between the antenna and the satellite. Furthermore, for static reference stations, because the GPS orbit period is approximately twice the rotation rate of the Earth, the relative geometry repeats every sidereal day. It was in this environment that Evans first noticed multipath [7]. His observation that the repeatability of multipath can be exploited by creating templates has lead to a number of investigations and applications.

The performance of template techniques is limited. Many schemes rely on the day-to-day repeatability of multipath. Studies have shown that templates perform more reliably when the true satellite period is utilized [8], [9] . When the templates are formed from measurement differences, then biases derived from the measurements involved are present.

The Dual Frequency Method (DFM) is a technique that simultaneously solves the problem of biases and timing associated with multipath templates[10]. In the DFM, templates are defined using an antenna-centered or *topocentric* coordinate system. In the case where multipath reflections are generated by predominantly local reflectors, and the local environment does not change, topocentric maps can provide an effective means to mitigate multipath [Cohen dissertation]. Therefore because the DFM correlates multipath to local coordinates, the technique does not suffer timing issues. Furthermore, the DFM solves for the biases associated with the observation of multipath by first organizing linear combinations by overhead pass. Where overhead passes intersect, the observations of multipath are differenced, forming a measurement of the difference in the respective biases. Over a long span of data collection, the set of bias difference evaluations is greater in number than the number of overhead passes. As the problem of solving the bias differences is overdetermined, then those bias differences can be solved in batch using a least squares estimate.

A GENERALIZED DUAL FREQUENCY METHOD

As originally developed the DFM provides a useful technique for not only evaluating multipath at a reference site but also for mitigating it [10]. However the DFM can be further extended in two ways. First, the combination of measurements prescribed in the original DFM can be generalized to a large family of differences. That family grows with each additional observable available to the user. This includes observables generated from modernized signals such as L2C. This could also include signals tracked in common among collocated receivers. A second extension to the DFM involves its search for the intersections of overhead passes, which is a computationally expensive process. A simplified model for predicting the intersections can be derived. The following sections are a partial restatement of the DFM process with an emphasis on these two prescribed extensions.

Observation Equations

The following equations can be used to model the observations derived from the tracking of a code x on a frequency f.

$$\rho = d + c\delta t + i_f + t + \nu + M + b_{IF} + b_x + \epsilon \qquad (1)$$

$$\phi = d + B_\phi + c\delta t - i_f + t + \nu + m + b_{IF} + \eta \qquad (2)$$

Each variable in Equations 1 and 2 represents either a distance or an error source in the observations. For the

purpose of clarity, each variable is not subscripted to fully identify its scope. For example, some variables are common to a frequency in general, where others may be satellite or receiver specific. Therefore the scope of each variable is described in the following text.

The variable ρ denotes a generalized pseudorange measurement. The variable ϕ is used to denote carrier phase. The units of carrier phase are here noted as a distance. The ambiguity in both whole and fractional cycles is represented by B_ϕ.

The true distance traveled from satellite phase center to receiver antenna phase center is represented by d. Some authors refer to this as the geometric distance. However, even in an inertial frame, the GPS signal bends by a few millimeters as it passes through the Earth's atmosphere and gravity well.

The difference in time offset between the receiver and a satellite is represented by the variable δ_t.

The path-dependent delay due to refraction by the ionosphere is denoted with i_f. The carrier phase is advanced by the same amount [11]. A linear relation described in Equation 3 exists between the ionosphere delay between the frequencies of L1 and L2.

$$i_{L2} = \gamma i_{L1} \tag{3}$$

The above linear relation is derived from the fact that ionosphere delay varies with the inverse square of the frequency. In this case the value of γ can be solved in Equation 4.

$$\gamma = \left(\frac{f_{L1}}{f_{L2}}\right)^2 \approx 1.65 \tag{4}$$

As more frequencies are introduced to GPS, additional linear relations can be formed.

Troposphere delay is denoted using t.

Special and general relativity corrections are represented by the variable ν . Multipath error in code and carrier phase observations are represented by the variables M and m, respectively.

Channel bias is represented using the variable b_{IF}. The channel bias represents the cumulative delay of the signal as it passes through antenna and receiver circuitry to the receiver's A/D sampler. That bias is difficult to observe in an absolute sense. However the difference of channel biases can be solved for among signals derived from the same receiver. In typical GPS user equipment, the path delay is common for all observations on L1, and for all observations on L2. Receivers that implement L2C or signals on L5 are likely to use additional electrical paths and thereby incur additional channel biases. It is also conceivable that receivers implement one channel per satellite in track. Finally, a future generation of software receivers may implement direct sampling of the L band. Because direct sampling uses one electrical path, such software receivers would also share a common, single bias.

Code bias is denoted using the variable b_x. This bias derives from the observation by the authors that pseudoranges estimated from different pseudocodes have a bias that is satellite dependent. The code bias is likely due to the imperfect autocorrelation of the pseudorandom codes. Similar biases could occur between other observables such as carrier phase and Doppler however for the purposes of this investigation are omitted.

Thermal noise is represented in code and phase using the symbols ϵ and η, respectively. The noise is not only Gaussian in nature, but also white.

A Family of Multipath Combinations

The observations are combined linearly to first expose multipath errors and then to remove the effect of the ionosphere delay. Each step requires the calculation of a difference or *divergence*. The family of possible divergences is large.

Figure 2 is a nodal graph that depicts the set of unique divergences that can be used for either multipath or for ionosphere delay. Each observable that can be derived from a receiver is marked with a colored, circular node. Light blue nodes represent time delay or pseuodorange observables. Light green nodes represent carrier phase observables. It is not possible to distinguish between these nodes using data recorded in the RINEX version 2 formats. However the proposed RINEX 3.00 standard provides the ability to make this distinction [12].

The lines that connect nodes represent unique divergences. Red lines represent divergences between frequencies. Blue lines represent divergences between observables that share a frequency. Green lines represent divergences between similar observables on a shared frequency.

The nodal graph is specific to a given receiver or configuration of receivers, as the types of codes, frequencies, and observables can vary from design to design. The graph in Figure 2 applies to single, hypothetical receiver that can simultaneously track C/A and P codes on L1, and L2C and P codes on L2.

There are two steps in forming each linear combination: a first divergence, and, if necessary, a second divergence to solve for ionosphere delay. The final combination will be dominated by multipath, a bias, and noise. The following variable μ will be used to denote in a general sense any of these combinations.

As a function of time and space, then μ follows Equation 5.

$$\mu = m(a, e) + B_\mu + \xi(t) \tag{5}$$

In Equation 5 μ is the sum of three variables: a multipath value m that is strictly a function of azimuth a and elevation e, a constant bias B_μ, and a thermal noise term $\xi(t)$.

The process can be illustrated with an example. Consider a receiver that tracks P code on L1 and L2C code. Then the

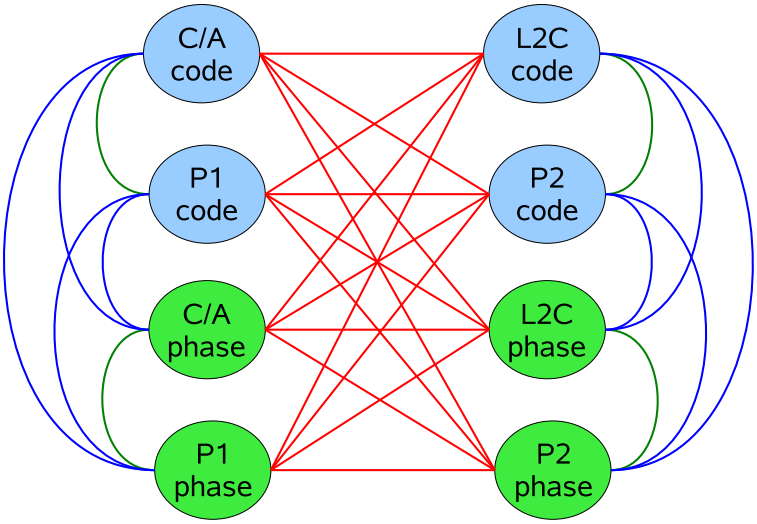

Fig. 2 Visualization of divergence combinations when tracking C/A, P code and L2C

observations equations realized for this case take the form of Equations 6 and 8.

$$\begin{aligned}
\rho_{L2C} &= d + c\delta t + \gamma i + t + \nu + M_{L2C} + b_{L2C} + \Delta_b \\
&\quad + \epsilon_{L2C} \qquad (6)\\
\phi_{P1} &= d + B_1 + c\delta t - i + t + \nu + m_{P1} + \eta_{P1} \qquad (7)\\
\phi_{L2C} &= d + B_2 + c\delta t - \gamma i + t + \nu + m_{L2C} \\
&\quad + \Delta_b + \eta_{L2C} \qquad (8)
\end{aligned}$$

Some simplifications have been made compared to Equations 1 and 2. Ionosphere delay on the frequency L1 is simply noted with the variable i. Similarly the channel biases are represented with a single variable on L2, Δ_b. The carrier phase ambiguities of the phases derived from P1 and L2C are noted as B_1 and B_2, respectively. There are no ionosphere free combinations of just two observable available for this hypothetical receiver. Therefore two divergences are required: $\Delta_1 = \rho_{L2C} - \phi_{L1}$ and $\Delta_2 = \phi_{P1} - \phi_{L2C}$. The divergences are stated in Equations 9 and 10.

$$\begin{aligned}
\Delta_1 &= \Delta B - B_1 + (\gamma + 1)i + M_{L2C} - m_{P1} \\
&\quad + b_{L2C} + \eta_{L2C} - \nu_{P1} \qquad (9)\\
\Delta_2 &= B_1 - B_2 + (\gamma - 1)i + m_{P1} - m_{L2C} \\
&\quad - \Delta_b + \nu_{P1} - \nu_{L2C} \qquad (10)
\end{aligned}$$

A single combination in the form of Equation 5 can now be formed with the following values.

$$m(a,e) = M_{L2C} - \frac{\gamma}{\gamma - 1} m_{P1} + \frac{1}{\gamma - 1} m_{L2C}$$

$$B_\mu = \Delta_b - B_1 - \frac{1}{\gamma - 1}(B_1 - B_2 - \Delta_b)$$

$$\xi(t) = \epsilon_{L2C} - \eta_{P1} - \frac{1}{\gamma - 1}(\eta_{P1} - \eta_{L2C})$$

The following are three more concrete examples of multipath combinations derived using this generalized process.

$$\mu_1 = \rho_{P1} - \phi_{P1} - \frac{2}{\gamma - 1}(\phi_{P1} - \phi_{P2})$$

$$\mu_2 = \rho_{C1} - \phi_{P1}$$

$$\mu_3 = \phi_{P1} - \phi_{P2} + \frac{1}{\gamma - 1}(\phi_{C1} - \phi_{P2})$$

The number of possible multipath combinations can be estimated for the hypothetical receiver depicted in Figure 2. The calculations are listed in Equations 11 to 15.

$$N_d = C(8,2) = \frac{8!}{2!(8-2)!} = 28 \qquad (11)$$

$$N_{if} = 4 \qquad (12)$$

$$N_{ic} = N_d - N_{if} = 24 \qquad (13)$$

$$N_{tc} = N_{ic} \cdot (N_{ic} - 1) = 24 \cdot 23 = 552 \qquad (14)$$

$$N_{mc} = N_{if} + Ntc = 556 \qquad (15)$$

The first step is to use combinatorics to form the total number of possible first divergences N_d. The number of first divergences free of ionosphere noted as N_{if}. The remaining combinations N_{ic} can be used to isolate either ionosphere or multipath but not both in order to ensure observability. Then the total number of multipath combinations that must be corrected for ionosphere is N_{tc}. Finally,

the total number of ionosphere corrected and ionosphere free combinations are summed in Equation 15. Note that this count of combinations is minimum number of unique combinations. For example, more than one second divergence could be combine to produce an improved estimate of ionosphere error.

Bias Estimation and Removal Using Overhead Pass Intersections

The key to the DFM is finding points in overhead geometry where two satellite passes, j and k, cross. The multipath for the two passes at a crossover point must be the same. By forming the difference in μ for each satellite at that point, the difference B_μ can be formed between passes j and k.

The following formulation repeats what is found in the original paper describing the DFM [10], with some simplifications.

For each intersection i, between passes j and k, the following differenced μ in Equation 16 can be formed..

$$y_i = \mu_j - \mu_k = B_{\mu,j} - B_{\mu,k} + \xi_j - \xi_k \qquad (16)$$

By collecting for each intersection an overdetermined set of equations can be formed with the matrix formulation in Equation 17.

$$y_{m\times 1} = H_{m\times n} x_{n\times 1} + \xi_{m\times 1} \qquad (17)$$

The total number of intersections found is m and the total number of passes is n. Each row in y corresponds to one intersection. The matrix elements of Equation 17 are defined by the terms in Equation 16.

$$\begin{aligned} y_i &= \mu_j - \mu_k & x_l &= \Delta B_{phi,1} - \Delta B_{phi,l} \\ H_{i,j} &= 1 & H_{ik} &= -1 \\ \xi_i &= \xi_j - \xi_k \end{aligned}$$

The matrix H as formed is rank deficient. By partitioning the above matrix equation to remove the first entry of x, a least squares solution becomes possible.

$$\left[\begin{array}{c} y_1 \\ \hline y_2 \\ \vdots \\ y_m \end{array}\right] = \left[\begin{array}{c|ccc} h_{11} & h_{12} & \cdots & h_{1n} \\ h_{21} & h_{22} & & \\ \vdots & & \ddots & \\ h_{m1} & & & h_{mn} \end{array}\right] \left[\begin{array}{c} x_1 \\ \hline x_2 \\ \vdots \\ x_n \end{array}\right] + \left[\begin{array}{c} \xi_1 \\ \hline \xi_2 \\ \cdots \\ \xi_m \end{array}\right] \qquad (18)$$

$$\left[\begin{array}{c} y_1 \\ \hline y' \end{array}\right] = \left[\begin{array}{c|c} h_{11} & \\ h_{21} & \\ \vdots & H' \\ h_{m1} & \end{array}\right] \left[\begin{array}{c} x_1 \\ \hline x' \end{array}\right] + \left[\begin{array}{c} \xi_1 \\ \hline \xi' \end{array}\right]$$

$$y'_{m\times 1} = H'_{m\times n-1} x_{n\times 1} + \xi_{m-1\times 1} \qquad (19)$$

The least squares solutions can then be stated in Equation 20

$$\hat{x}' = (H'^T H')^{-1} H'^T y' \qquad (20)$$

Analytic Solution to the Overhead Pass Intersection Search

Prior applications of the DFM have used a numerical search to find the intersection of overhead passes. However an analytic solution is possible. The key to the analytic solution is to adopt a simple model of satellite orbital motion, then to take advantage of symmetries in that model.

In the Earth centered, inertial (ECI) frame, a first order model for the orbit of each GPS satellites is an inclined circular orbit, with a constant radius. When that orbit is transformed into the Earth centered, Earth fixed (ECEF) frame, the orbit becomes a three-dimensional Lissajous figure. Because the axis of rotation of the Earth coincides with the axis of rotation of the satellite, then the satellite path can be seen as confined to a sphere in the ECEF frame. In Figure 3 the equivalency of the sphere in the two frames can be seen.

The orbits of two satellites become two curves on the ECEF sphere. The intersection between any two curves occurs at two points. When either of those points are viewed from the surface of the Earth, they necessarily are the points of intersections for an overhead pass. *Therefore orbit intersections solved in the ECEF frame correspond to intersections in the topocentric frame.*

The orbits traced on this sphere also can be related to groundtracks. As a satellite orbits the Earth, the point where the satellites position vector intersects with the surface of the Earth is referred to as the subsatellite point. Over time, the line traced by subsatellite points is the groundtrack. Therefore lines of the sphere containing the GPS satellite orbits are scaled replicas of the respective groundtracks. *Then intersections in the ECEF and ECI frames correspond to intersections of ground tracks.* The analytic solution to the intersection search can then draw from the spherical trigonometry associated with ground tracks [13].

However, most models of ground tracks are parametric in time. An analytic solution to the intersection problem requires that the ground tracks be parameterized in terms of a geometry quantity. For these circular orbits the *argument of latitude* U ties geometry with time.

Figure 4 depicts satellite motion in an inertial frame. That inertial frame is coincident with the ECEF frame at a particular epoch–midnight at the beginning of the GPS week. This is the ECEF frame in which the broadcast GPS ephemeris is transmitted [14]. The angle from the equator along the orbit plane to the satellite is U. The latitude at which the satellite crosses the equator is Λ. This set of angular parameters is sufficient to solve the intersection problem.

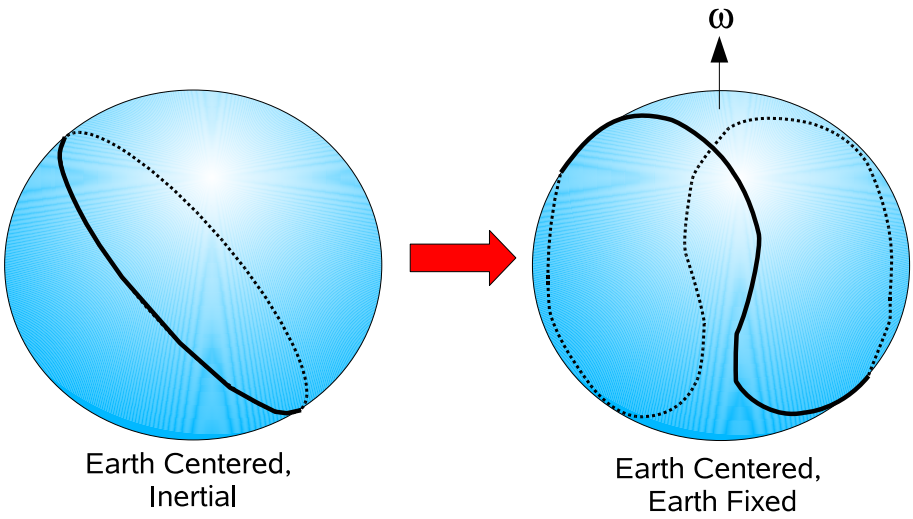

Fig. 3 Using simplified dynamics, the GPS satellites are confined to a sphere in both the ECI and ECEF frames.

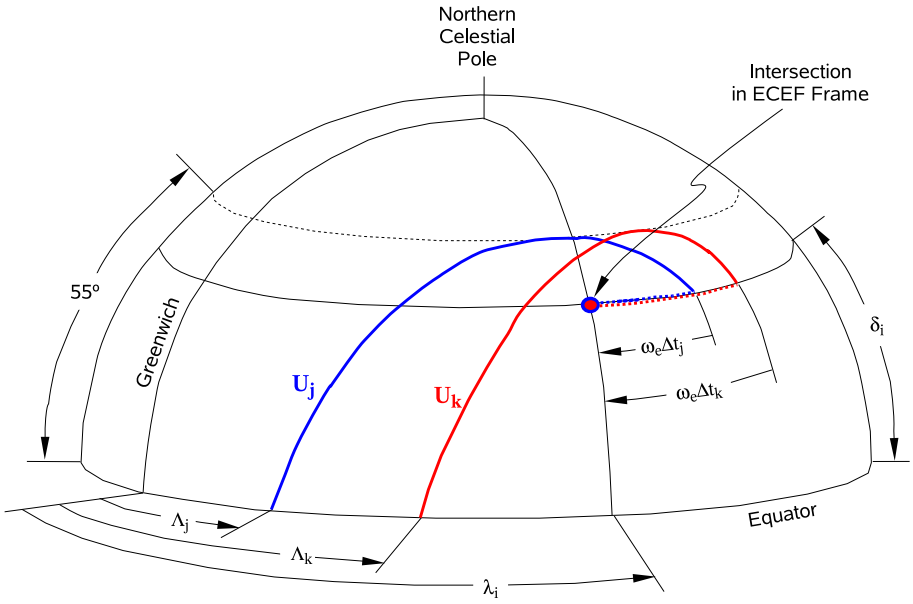

Fig. 4 Spherical geometry relating satellite position in the ECI to ECEF frames.

Because GPS has a repeating ground track, Λ is a constant for each satellite. Λ can be computed from a GPS ephemeris. Equations 21 through 24 state the relationship between Λ and the standard Keplerian parameterization of the GPS ephemeris.

$$n = \sqrt{\frac{\mu}{a^3}} \tag{21}$$

$$t_{AN} = \frac{2\pi - M_0 - \omega}{n} \tag{22}$$

$$\Omega' = \Omega_0 - \omega_e \cdot t_{oe} \tag{23}$$

$$\Lambda = \Omega' - \omega_e t_{AN} \tag{24}$$

The point of intersection is defined by two angles, a longitude λ_i and a latitude δ_i. Using symmetry it can be shown that the points of intersection for satellites i and j are found on the great circle defined by Equation 25.

$$\lambda_i = \frac{\Lambda_j + \Lambda_k}{2} + \frac{\pi}{4} \tag{25}$$

The motion of the satellite on this sphere forms the spherical triangle depicted in Figure 5. The shape ABC is a spherical triangle with one right angle at the C vertex. The angle formed at vertex A is the inclination of the orbit plane i. Because the orbit rate of the GPS satellites is twice the sidereal rotation rate of the Earth, the substitution $\omega_e \Delta t = \frac{U}{2}$ can be made. Based on this configuration, Equations 26 and 27 must be solved implicitly for the two unknowns U and δ_i.

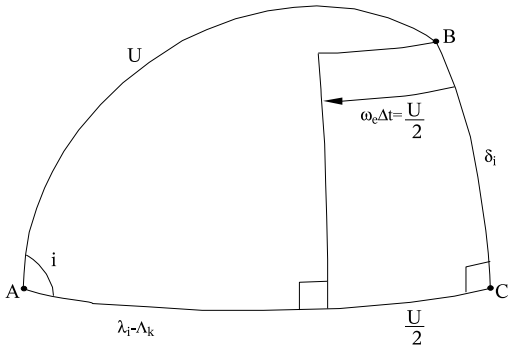

Fig. 5 Spherical triangle relating argument of latitude to ECEF latitude and longitude.

$$\cos U = \cos\left(\lambda - \Lambda + \frac{U}{2}\right) \tag{26}$$

$$\sin U \sin i = \sin \delta_i \tag{27}$$

APPLICATION

Using `mpsolve`

The open source application `mpsolve` can be used to evaluate the multipath in a given environment. It can also be used to explore the family of multipath combinations. The program is part of the GPSTk [15].

The simplest function of `mpsolve` is to generate statistics for a site based on an input RINEX observation or navigation file. The default combination used by `mpsolve` is given in the following

$$\mu_1 = \rho_{P1} - \phi_{L1} - \frac{2}{1-\gamma}(\phi_{L1} - \phi_{L2}) \tag{28}$$

As of this writing `mpsolve` can either generate second order statistics (standard deviation) of a multipath combination, sorted into bins of either azimuth or elevation, or list the raw combinations to be further processed by the user. Second order statistic are required as multipath combination, and their means, are biased. A full implementation of the DFM is targeted as a future enhancement to `mpsolve`.

The default behavior is to report a list of statistics binned by elevation. Figure 6 shows an example run:

```
~/svn/gpstk/dev/apps/multipath:
> ./mpsolve -o arl_255.06o -e arl_255.06n
Multipath Environment Evaluation Tool

Edited 1176 points (4.3%).
Overhead passes used: 65

Standard deviation of bins sorted by
  elevation.

From   0 to  90: 0.65
From  10 to  30: 0.763
From  20 to  40: 0.568
From  40 to  90: 0.249
From  10 to  90: 0.546

Total points used: 25988
         rejected: 0
```

Fig. 6 Basic output from `mpsolve`

Multiple input RINEX observation and navigation files can be specified by repeating the '-o' and '-e' options, respectively. Statistics can be presented by bins, or the raw data can be dumped via the '-r' option. Figure 7 shows example output from the -r option.

The output can be optionally formatted for input into numerical packages using the '-n' option. This holds true whether statistics or raw data is output. Figure 8 demonstrates the numerical mode of `mpsolve`.

The user can specify the multipath combination or use the default. Figure 9 is an example of a combination dominated by multipath on L2.

The user defined expression in theory could be any combination of observable: "P1-C1", "L1-L2". The observable names out of the RINEX header are used as placeholders. Nonlinear functions like sine, log base 10, etc., are available too.

```
> ./mpsolve -o arl_255.06o -e arl_255.06n -r
Multipath Environment Evaluation Tool

Edited 1176 points (4.3%).
Overhead passes used: 65
09/12/2006 00:00:00 GPS 4 Pass 0 24894794.3406
09/12/2006 00:00:00 GPS 8 Pass 1 25709933.2373
09/12/2006 00:00:00 GPS 11 Pass 2 25168300.1083
09/12/2006 00:00:00 GPS 17 Pass 3 25373340.2647
09/12/2006 00:00:00 GPS 24 Pass 5 24801829.8059
09/12/2006 00:00:00 GPS 26 Pass 6 24853157.3703
09/12/2006 00:00:00 GPS 27 Pass 7 25769822.3835
09/12/2006 00:00:00 GPS 28 Pass 8 25594402.803
09/12/2006 00:00:00 GPS 29 Pass 9 25763495.3664
09/12/2006 00:00:30 GPS 4 Pass 0 24894794.3107
09/12/2006 00:00:30 GPS 8 Pass 1 25709933.9599
09/12/2006 00:00:30 GPS 11 Pass 2 25168299.3041
09/12/2006 00:00:30 GPS 17 Pass 3 25373339.946
09/12/2006 00:00:30 GPS 24 Pass 5 24801829.5413
09/12/2006 00:00:30 GPS 26 Pass 6 24853156.6907
09/12/2006 00:00:30 GPS 27 Pass 7 25769821.195
```

Fig. 7 Raw combination can be listed by `mpsolve`.

```
./mpsolve -o arl_255.06o -e arl_255.06n -r -n
# GPS Week, Seconds of week, Sat. id,
# Sat. system, Pass, Multipath value,
# LLI indicator
1392 172800 4 1 0 24894794.3406 0
1392 172800 8 1 1 25709933.2373 0
1392 172800 11 1 2 25168300.1083 0
1392 172800 17 1 3 25373340.2647 0
1392 172800 24 1 5 24801829.8059 0
1392 172800 26 1 6 24853157.3703 0
1392 172800 27 1 7 25769822.3835 0
1392 172800 28 1 8 25594402.803 0
1392 172800 29 1 9 25763495.3664 0
1392 172830 4 1 0 24894794.3107 0
1392 172830 8 1 1 25709933.9599 0
1392 172830 11 1 2 25168299.3041 0
```

Fig. 8 Raw combinations in numeric form.

```
mpsolve -m "P2-wl1*L2+2/(1-gamma)*(wl1*L1-wl2*L2)"
  -o arl_255.06o -e arl_255.06n
```

Fig. 9 The user can define a new expression for mpsolve to evaluate for each satellite and epoch.

RESULTS

A New Family of Multipath Combinations

Numerous tests of `mpsolve` have demonstrated that a difference formed using the prescribed method is dominated by multipath and only a simple bias per pass. The reader has the ability to acquire `mpsolve` as part of the GPSTk [16] and process RINEX observations to confirm that these families of observations exist and they provide valuable information about new reference station sites and receivers.

As a demonstration of the spatial consistency associated with a simple alternative combination, a long term set of observations was processed using `mpsolve` and plotted as a polar grid in Figure 10. The radius corresponds to elevation. The angle from the vertical direction to the right is azimuth. The DFM solution that resolved biases among the passes was scripted in Octave [17]. These are the differences of $\rho_{C1} - \rho_{P1}$, spanning GPS weeks 1303 to 1350, the majority of the year 2005. The receiver that took these observations was an Ashtech Z/Y-12. While the solutions seem consistent overall, there are a few outliers that skewed the range of the plot into tens of meters before they were edited.

Confirmation of the Intersection Search

At the time of this writing, an implementation of the DFM has not been implemented within `mpsolve`. However the GPSTk application `wheresat` does generate satellite positions as a function of time. The satellite positions generated are in ECEF coordinates and, upon user selection, in topocentric coordinates [18]. Manual inspection confirms that when GPS satellites intersections occur, the ECEF coordinates converge.

Based on this inspection, the prescribed analytic solution has the potential to produce intersection solutions that agree with the numerical solution to within fractions of a degree, when measured with azimuth and elevation. However that difference can grow large to even 2 degrees as satellites vary from the nominal GPS orbit. More study is required to sufficiently compare the results of a numerical and analytic solution.

CONCLUSIONS AND FUTURE WORK

As GPS modernization and Galileo become a reality, researchers are faced with the challenge of assessing strategies to take advantage of the new signals. The generalized DFM offers one method to compare the relative quality of signals using field measurements instead idealized models. By using a variety of multipath combinations, the multipath resistance of new signals or new receivers can be systematically compared to those already in existence. The

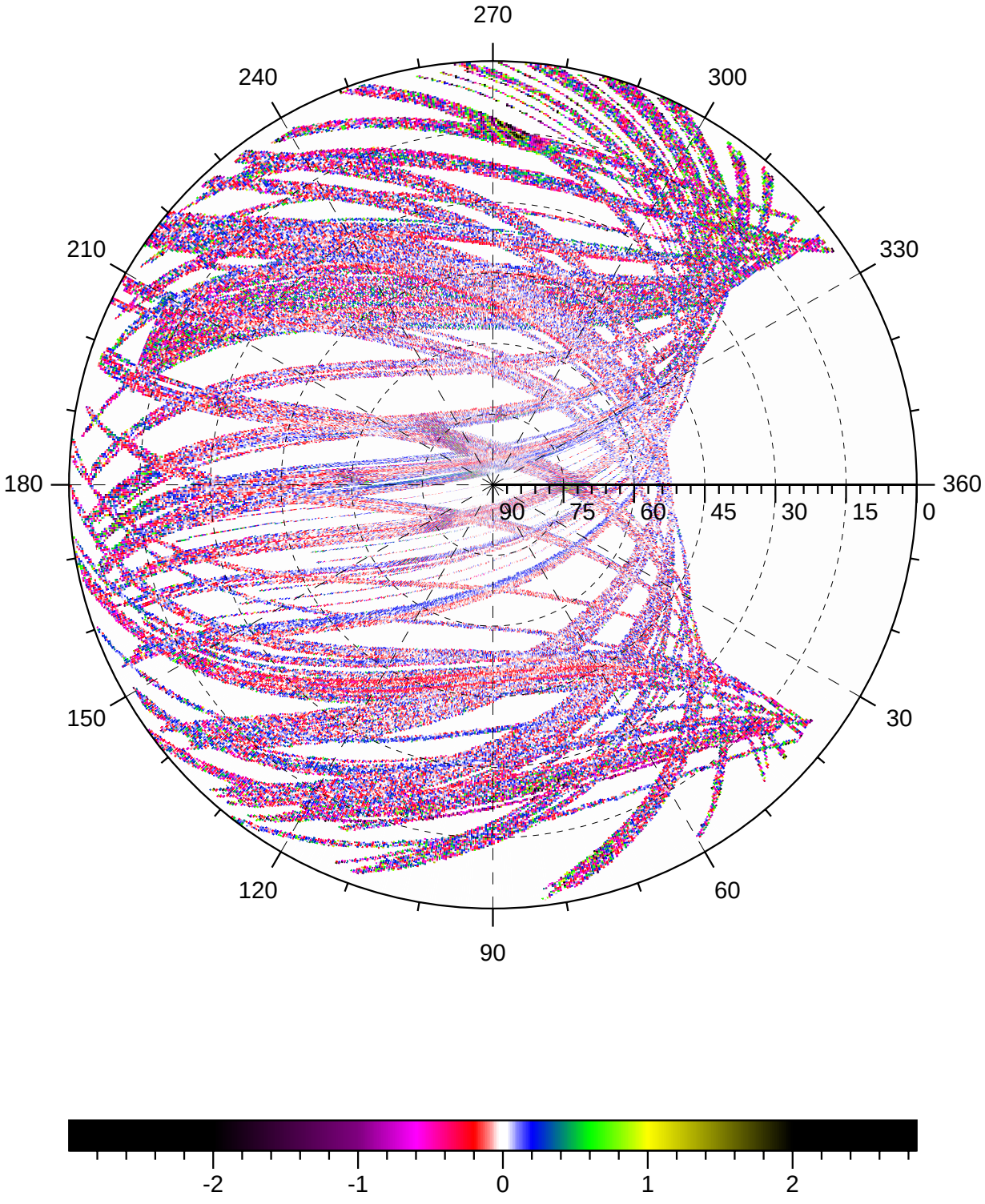

Fig. 10 Long term DFM solution to C/A minus Z/Y code on L1.

GPSTk program `mpsolve` provides a convenient application to compute and to report the results multipath combinations.

The accuracy of the intersection solution is the next step associated with the development of the generalized DFM. While the concept has been proven looking at specific data sets, a systematic evaluation is neccessary to confirm that this new method does not affect the results of the DFM.

The application of the DFM to new signals and new systems, and its full implementation within `mpsolve`, is a work in progress. Like many open source applications, and GPS itself, the users play a significant role in its evolution.

ACKNOWLEDGEMENTS

The authors would like to thank Applied Research Laboratories, The University of Texas at Austin, for its support of research to empirically model multipath, and in its support of the GPS Toolkit.

REFERENCES

[1] Kenn Gold and Alison Brown. An array of digital antenna elements for mitigation of multipath for carrier landings. In *Proceedings of the Nation Technical Meeting of the Institude of Navigation*, San Diego, California, January 2005.

[2] Richard van Nee, Bryan Townsend, Patrick Fenton, and Keith Van Dierendonck. L1 carrier phase multipath error reduction using medll technology. In *Proceedings of the 8th International Technical Meeting of the Satellite Division of the Institute of Navigation*, Palm Springs, California, September 1995.

[3] Lionel Garin, Frank van Diggelen, and Jean-Michel Rousseau. Strobe and edge correlator multipath mitigation for code. In *Proceedings of the 9th International Technical Meeting of the Satellite Division of the Institute of Navigation*, Kansas City, Missouri, September 1996.

[4] Lawrence Weill. Achieving theoretical accuracy limits for pseudoranging in the presence of multipath. In *Proceedings of the 8th International Technical Meeting of the Satellite Division of the Institute of Navigation*, Palm Springs, California, September 1995.

[5] Susan Gomez, Robert Panneton, Penny Saunders, Shian Hwu, and Ba Lu. Gps multipath modeling and verification using geometrical theory of diffraction. In *Proceedings of the 8th International Technical Meeting of the Satellite Division of the Institute of Navigation*, Palm Springs, California, September 1995.

[6] Roberto V. F. Lopes and Paulo G. Milani. Consistent on-board multipath calibration for gps-based spacecraft attitude determination. In *Proceedings of the 13th International Technical Meeting of the Satellite Division of the Institute of Navigation*, Salt Lake City, Utah, September 2000.

[7] Alan G. Evans. Comparison of gps pseudorange and biased doppler range measurements to demonstrate signal multipath effects. In *Proceedings of the 4th International Geodetic Symposium on Satellite Positioning*, Austin, Texas, April 1986.

[8] James Stafford. A practical technique for assessing multipath mitigation methods for dgps applications. In *Proceedings of the 11th International Technical Meeting of the Satellite Division of the Institute of Navigation*, Nashville, Tennessee, September 1998.

[9] Penina Axelrad, Kristine Larson, and Brandon Jones. Use of the correct satellite repeat period to characterize and reduce site-specific multipath errors. In *Proceedings of the 18th International Technical Meeting of the Satellite Division of the Institute of Navigation*, Long Beach, California, September 2005.

[10] Changdon Kee and Bradford Parkinson. Calibration of multipath errors on gps pseudorange measurements. In *Proceedings of the 7th International Technical Meeting of the Satellite Division of the Institute of Navigation*, Salt Lake City, Utah, September 1994.

[11] Pratap Misra and Per Enge. *Global Positioning Sytem: Signals, Measurements and Performance*. Ganga-Jamuna Press, Lincoln, Massachusetts, 2004.

[12] Werner Gürtner and Lou Estey. *RINEX: The Reciever Independant Exchange Format Version 3.00*. ftp://igscb.jpl.nasa.gov/igscb/data/format/rinex300.pdf, 2006.

[13] Wiley J. Larson and James R. Wertz, editors. *Space Mission Analysis and Design*. Microcosm, Inc., and Kluwer Academic Publishers, 1988.

[14] *NAVSTAR Global Positioning System Interface Specification (IS-GPS-200), Revision D*.

[15] R. Benjamin Harris, Brian Tolman, Tom Gaussiran, David Munton, Jon Little, Richard Mach, Scot Nelsen, and Brent Renfro. The GPS Toolkit: Open Source GPS Software. In *Proceedings of the 17th International Technical Meeting of the Satellite Division of the Institute of Navigation*, Long Beach, California, September 2004.

[16] GPSTk website. http://www.gpstk.org/.

[17] Octave website. http://www.octave.org/.

[18] R. Benjamin Harris, Timothy Craddock, Tracie Conn, Thomas Gaussiran, Eric Hagen, Anthony Hughes, Jon Little, Richard Mach, Scot Nelsen, Brent Renfro, and Brian Tolman. Open signals, open software: Two years of collaborative analysis using the gps toolkit. In *Proceedings*

of the 19th International Technical Meeting of the Satellite Division of the Institute of Navigation, Fort Worth, Texas, September 2006.